

*Methods Article*

## Simplified, Cost Effective, and Accurate Calculation of Critical Wavelength via the MATLAB Software

### *Article History*

**Received:** 20 March 2021;

**Received in Revised Form:** 25 April 2021;

**Accepted:** 27 April 2021;

**Available Online:** 4 May 2021

**Camille Keisha Mahendra<sup>1\*</sup>, Cayvern Kishen Mahendra<sup>1</sup>, Priya Pusparajah<sup>2</sup>, Thet Thet Htar<sup>1</sup>, Lay-Hong Chuah<sup>1</sup>, Acharaporn Duangjai<sup>3,4</sup>, Tahir Mehmood Khan<sup>1,5</sup>, Yoon-Yen Yow<sup>6</sup>, Yatinesh Kumari<sup>7</sup>, Bey Hing Goh<sup>1,8,9\*</sup>**

<sup>1</sup>Biofunctional Molecule Exploratory Research Group, School of Pharmacy, Monash University Malaysia, 47500 Bandar Sunway, Selangor Darul Ehsan, Malaysia, camille.mahendra@monash.edu; cayvern.kishen@gmail.com; Thet.Thet.Htar@monash.edu; Alice.Chuah@monash.edu; Goh.Bey.Hing@monash.edu

<sup>2</sup>Medical Health and Translational Research Group, Jeffrey Cheah School of Medicine and Health Sciences, Monash University Malaysia, 47500 Bandar Sunway, Selangor Darul Ehsan, Malaysia, Priya.Pusparajah@monash.edu

<sup>3</sup>Center of Health Outcomes Research and Therapeutic Safety (Cohorts), School of Pharmaceutical Sciences, University of Phayao, Phayao, Thailand, achara.phso@gmail.com

<sup>4</sup>Division of Physiology, School of Medical Sciences, University of Phayao, Phayao, Thailand, achara.phso@gmail.com

<sup>5</sup>Institute of Pharmaceutical Sciences (IPS), University of Veterinary & Animal Sciences (UVAS) Out Fall Road, Lahore 54000, Pakistan, tahir.khan@uvas.edu.pk

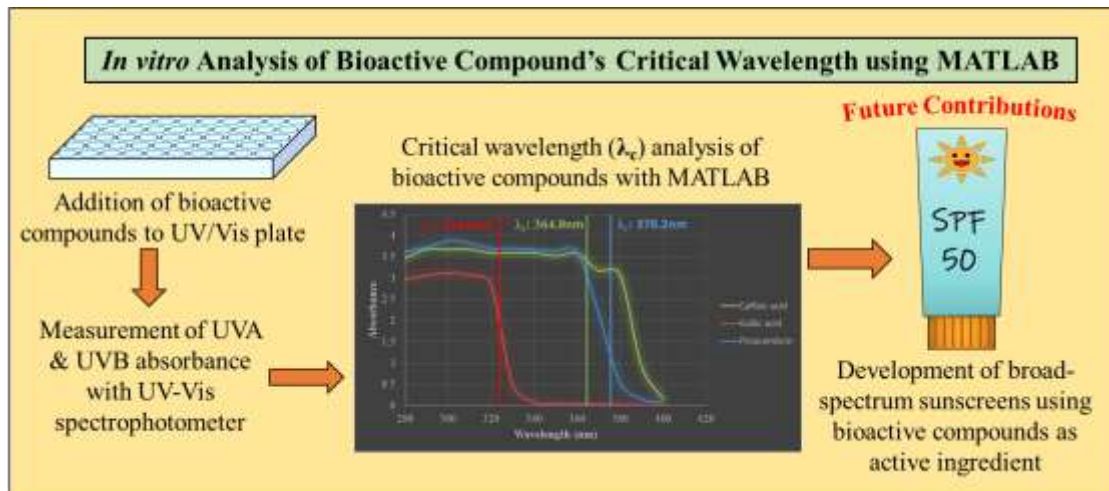
<sup>6</sup>Department of Biological Sciences, School of Science & Technology, Sunway University, Bandar Sunway 47500, Selangor Darul Ehsan, Malaysia, yoonnyeny@sunway.edu.my

<sup>7</sup>Jeffrey Cheah School of Medicine and Health Sciences, Monash University Malaysia, Bandar Sunway, Malaysia, yatinesh.kumari@monash.edu

<sup>8</sup>College of Pharmaceutical Sciences, Zhejiang University, 866 Yuhangtang Road, Hangzhou 310058, China

<sup>9</sup>Health and Well-Being Cluster, Global Asia in the 21st Century (GA21) Platform, Monash University Malaysia, Bandar Sunway 47500, Malaysia

\*Corresponding author: Camille Keisha Mahendra and Bey Hing Goh, School of Pharmacy, Monash University Malaysia, 47500 Bandar Sunway, Selangor Darul Ehsan, Malaysia; camille.mahendra@monash.edu and goh.Bey.Hing@monash.edu



**Abstract:** The use of sunscreens in our daily lives to reduce UV exposure on our skin is a good measure against photoaging. However, the current active ingredients in the market are not able to cover the entire spectrum range of UVA and UVB. Therefore, broader spectrum compounds are constantly being searched by cosmetic companies to replace the commercially available UV filters. In this study, an experimental model utilizing the MATLAB software was developed to measure a compound's critical wavelength ( $\lambda_c$ ). The purpose of this research was to ease the cost and speed up the screening of bioactive compounds for photoprotective properties while maintaining accuracy in the process. In this paper, the measurement of caffeic acid, gallic acid, and pinocembrin's critical wavelength in the MATLAB software was explained in a step-by-step guide. This was done to create an understandable and executable procedure for future researchers to utilize. Subsequently, from the results, the critical wavelength of caffeic acid, gallic acid, and pinocembrin was 378.2nm, 324.6nm, and 364.8nm, respectively. This shows that caffeic acid has the broadest absorbance spectrum, followed by pinocembrin, and finally gallic acid. Thus, it may be possible that caffeic acid might have stronger photoprotective abilities as compared to pinocembrin and gallic acid, based on its critical wavelength.

**Keywords:** Sunscreen; critical wavelength; MATLAB; UV rays; bioactive compounds

## 1. Introduction

Photoaging is the premature aging of the skin by ambient UV exposure and is characterized by the formation of wrinkles, irregular pigmentation, loss of skin resilience, etc.<sup>[1–3]</sup>. Therefore, many different kinds of sunscreens were developed by cosmetic companies as a protectant against the detrimental effects of UV rays. Sunscreens can be categorized into two different groups: physical (inorganic) and chemical (organic) sunscreens. Physical sunscreens, such as titanium dioxide and zinc oxide, reflect and scatter UV rays while chemical sunscreens absorb and dissipate high-intensity UV rays<sup>[4]</sup>. Chemical sunscreens can be further classified into two different categories based on their filter against UVA or UVB. Examples of UVA filters available in the market are benzophenones, dibenzoylmethanes, and anthranilates, while UVB

filters are *p*-aminobenzoic acid (PABA) derivatives, cinnamates, salicylates, and camphor derivatives<sup>[5]</sup>. These compounds are often used in combination as not one is broad enough in its absorbance spectrum nor high enough in sun protection factor (SPF) to completely negate the UV rays<sup>[5]</sup>.

Critical wavelength ( $\lambda_c$ ) is defined as the wavelength where the integral of the spectral absorbance curve is at 90% of the integral from 290–400 nm and the formula to determine it was developed by Diffey<sup>[6]</sup> as can be seen in Equation 1.

$$\int_{290}^{\lambda_c} A(\lambda)d\lambda = 0.9 \int_{290}^{400} A(\lambda)d(\lambda) \quad (1)$$

There are several benefits to this method in comparison to SPF measurement. Firstly, the measurement of critical wavelength is independent of application thickness because the measurement is inherently based on the absorbance curve instead of its amplitude. Secondly, the proposed method considers the electromagnetic spectrum from 290–400 nm as a single continuous entity, accounting for both UVA and UVB<sup>[7,8]</sup>. Thirdly, this method is conducted *in vitro*, removing the dangers, costs, and time consumption necessary for human clinical testing<sup>[9]</sup>. Next, for a sunscreen to hold the title of broad-spectrum, it must at least have a critical wavelength of 370 nm, which indicates, that a product is able to absorb the entire UVB range and some parts of UVA<sup>[9–11]</sup>. Although SPF is a popular measurement used to evaluate the photoprotective efficiency of a sunscreen against UV-induced skin erythema, FDA and ISO guidelines dictate that a product's critical wavelength must be measured and reported to best showcase a product's ability<sup>[10–11]</sup>. This is because the true value of SPF is easily affected by the amount applied to the skin. Despite being encouraged to apply up to 2 mg/cm<sup>2</sup> layer of sunscreen, many only apply up to a quarter of that amount in real life<sup>[12]</sup>. It had been reported that the SPF of the applied sunscreen significantly decreased when lesser amounts are applied to the skin<sup>[12,13]</sup>.

Therefore, in this study, the critical wavelength of three different bioactive compounds, caffeic acid, gallic acid, and pinocembrin, will be calculated using the MATLAB software as a case study. The use of bioactive compounds from natural sources is not only common in the medical field but is also widely used in cosmetic and agriculture products<sup>[14]</sup>. This is due to the increase in consumer demand towards more cost-saving, greener and sustainable sources<sup>[15]</sup>. In this study, the bioactive compounds (Figure 1) chosen were previously reported to have photoprotective properties. The photoprotective properties of caffeic acid were proven when the compound significantly protected the skin against UVB-induced erythema in human volunteers<sup>[16]</sup>. Additional molecular studies revealed that caffeic acid was able to inhibit the expression of MMP-1 and increase collagen production in UVB irradiated human fibroblast cells due to the suppression of reactive oxygen species (ROS) production in UVB irradiated cells and in turn suppressed the expression of NF- $\kappa$ B and phosphorylation of mitogen-activated protein kinases (MAPK) markers, which are triggers to MMP-1 expression<sup>[17,18]</sup>. This finding was

supported by another study which also showed that topical caffeic acid suppressed not only NF- $\kappa$ B expression but also cyclooxygenases-2 (COX-2), and prostaglandin E<sub>2</sub> (PGE<sub>2</sub>) by directly inhibiting Fyn kinase activity when tested on both *in vitro* and *in vivo* mouse skin cells<sup>[19]</sup>. Hence, through these studies, it can be seen that caffeic acid does possess photoprotective properties. On the other hand, in the study done by García Forero, *et al.*<sup>[20]</sup>, pinocembrin was reported to not only display maximum wavelength absorption within the UVC and UVB range but also increased the SPF *in vitro* values and inhibited DNA damage in both *E. coli* PQ37 strain and human embryo kidney (HEK-293) cells. Other studies on pinocembrin also displayed that the compound is able to inhibit oxidative stress in retinal pigment epithelium and inhibit the activation of nuclear factor (NF)- $\kappa$ B, degradation of I $\kappa$ B, and expression matrix metalloprotease (MMP)-1, 3, and 13 in human chondrocytes<sup>[21,22]</sup>. Although these two studies are not directly conducted on skin models, the cascade of UVB photoaging is also triggered by similar markers as described by Mahendra, *et al.*<sup>[17]</sup>, hence, suggesting that pinocembrin might potentially be able to suppress photodamage. Finally, gallic acid and its derivatives from green algae were suggested to contribute to the plant's photoprotective properties through its high antiradical activities<sup>[23]</sup>. Similar to caffeic acid, gallic acid also attenuate skin photoaging through the suppression of ROS production, which in turn decreased the expression of IL-6 and MMP-1 in UVB irradiated normal human dermal fibroblast. Topical application of gallic acid on hairless mice even shown that the wrinkles formation was much more superficial as compared to those irradiated by UVB. There was even an increase in hydration in the stratum corneum by 127% and a decrease in erythema index by 28% as compared to the UVB treated group<sup>[24]</sup>. Thus, based on these reports, these compounds were most suitable to showcase the accuracy and ease of using this experimental model and MATLAB software in evaluating the spectral absorbance curve and critical wavelength of each compound. Through this, we aim to develop an experimental model which will aid in easing the primary selection of natural products to be used as active ingredients in sunscreens. Here, the step-by-step process of using MATLAB to obtain the critical wavelength will be described in detail in this paper in hopes to provide future researchers with a template to perform similar studies or a general procedure to perform the analysis.

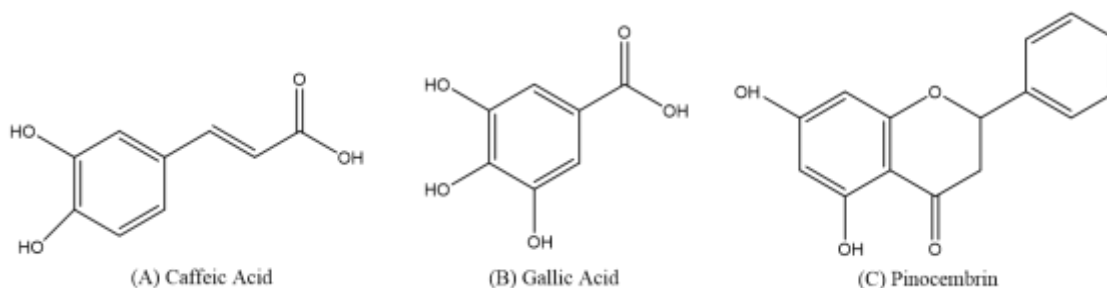


**Figure 1.** The chemical structure of photoprotective bioactive compounds. (A) Caffeic acid, (B) Gallic acid, and (C) Pinocembrin.

## 2. Methods and Materials

### 2.1. Materials

Bioactive compounds, gallic acid, pinocembrin, and caffeic acid, were obtained from Sigma Aldrich (St. Louise, USA) and prepared in 100% DMSO. Their absorbance spectrum was measured using a 96 well UV/Vis plate (Corning, USA) and UV spectrophotometer (Biotek, USA). The MATLAB software license in this study was subscribed by Monash University.

### 2.2. Obtaining Absorbance Spectrum

The absorbance of 20 mg/mL gallic acid, pinocembrin, and caffeic acid were measured from 290–400 nm using a UV/Vis plate in a UV spectrophotometer. As DMSO was used as the solvent in the preparation of the bioactive compounds, its absorbance was measured as well to act as the blank. After normalizing against the blank, the absorbance spectrum of each sample was evaluated using MATLAB.

### 2.3 Determining Critical Wavelengths

#### 2.3.1. Preparations

As a prerequisite to perform the following work, two software had to be installed. First being a software to store experimental data, which here, Microsoft Excel was used. Second being a programming software to analyze the data, such as MATLAB was used. Within MATLAB, the work was utilized using two working environments. One was the Editor for coding the main scripts and also function files. The other was a sub-application known as the Curve Fitting Toolbox to fit the scattered data to functions for calculation purposes.

#### 2.3.2 Importing data

The data for the absorbance spectrum for the bioactive compounds of interest is first to be extracted from Microsoft Excel. In this case, the bioactive compounds are caffeic acid, gallic acid, and pinocembrin. The data can be imported into MATLAB through various method. In this work, the *Import Data* function was used as can be seen in Figure 2. This will allow MATLAB to read and import data from the file of choice, in this case, “*uvb spectrum trial 2 110820.xlsx*”.



**Figure 2.** Navigation to Import Data from External Files.

The desired data was then highlighted to be imported. After importing, a temporary file will appear in the *workspace* as in Figure 3 and Figure 4.

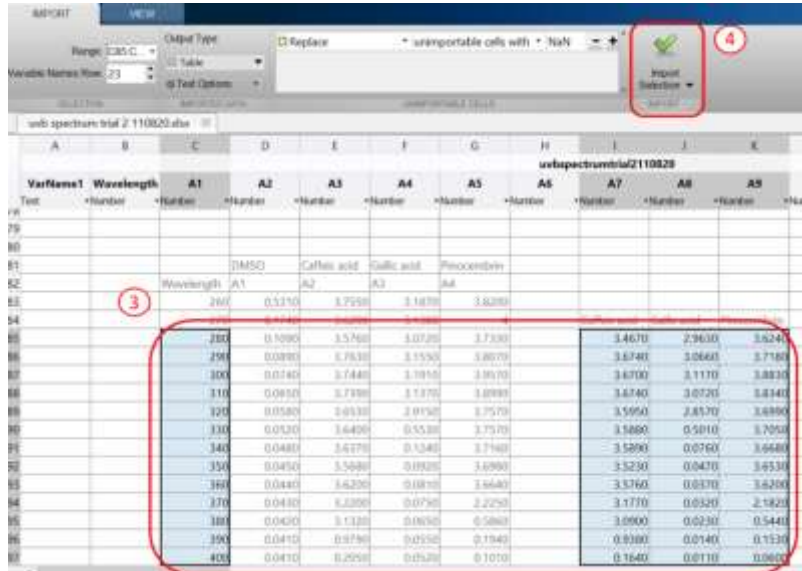
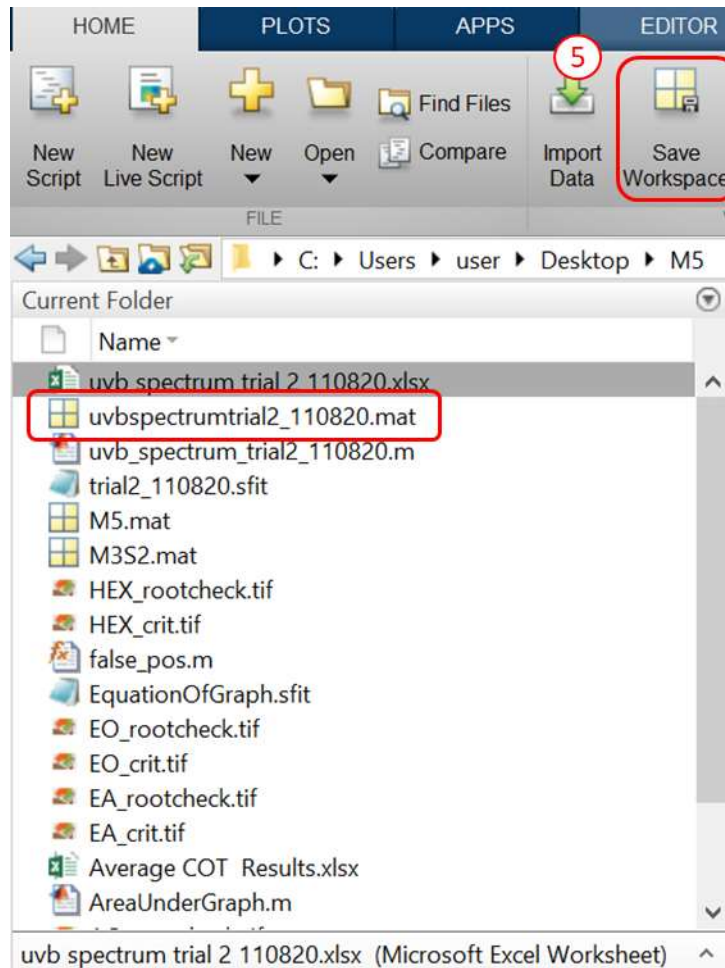


Figure 3. Selection of Desired Data to be Imported.



Figure 4. Temporary File in MATLAB Editor Workspace.

The temporary file was then saved as a *.mat* file – “*uvb\_spectrum\_trial2\_110820.mat*”, using the *Save Workspace* function as shown in Figure 5. Note that the file has to be saved into the same folder as the main script.



**Figure 5.** Generating *.mat* file using the Save Workspace Function.

Now, the saved *.mat* file can be loaded into the MATLAB Editor using the script below. After loading the file, variable names had been assigned accordingly in the MATLAB Editor as seen in Figure 6, with *wavelength* being the spectrum; *CA* being the absorbance of caffeic acid, *GA* being the absorbance of gallic acid, and *PC* being the absorbance of pinocembrin.

a)

|    | 1<br>A1 | 2<br>A7 | 3<br>A8 | 4<br>A9 |
|----|---------|---------|---------|---------|
| 1  | 280     | 3.4670  | 2.9630  | 3.6240  |
| 2  | 290     | 3.6740  | 3.0660  | 3.7180  |
| 3  | 300     | 3.6700  | 3.1170  | 3.8830  |
| 4  | 310     | 3.6740  | 3.0720  | 3.8340  |
| 5  | 320     | 3.5950  | 2.8570  | 3.6990  |
| 6  | 330     | 3.5880  | 0.5010  | 3.7050  |
| 7  | 340     | 3.5890  | 0.0760  | 3.6680  |
| 8  | 350     | 3.5230  | 0.0470  | 3.6530  |
| 9  | 360     | 3.5760  | 0.0370  | 3.6200  |
| 10 | 370     | 3.1770  | 0.0320  | 2.1820  |
| 11 | 380     | 3.0900  | 0.0230  | 0.5440  |
| 12 | 390     | 0.9380  | 0.0140  | 0.1530  |
| 13 | 400     | 0.1640  | 0.0110  | 0.0600  |

b)

```

1- load 'uvbspectrumtrial2_110820.mat'
2- wavelength = uvbspectrumtrial2_110820.A1;
3
4- CA = uvbspectrumtrial2_110820.A7; %Caffeic Acid
5- GA = uvbspectrumtrial2_110820.A8; %Gallic Acid
6- PC = uvbspectrumtrial2_110820.A9; %Pinocembrin

```

**Figure 6.** (a) The Data in *uvb\_spectrum\_trial2\_110820.mat* and (b) The Variable Assignment in MATLAB Editor.

### 2.3.3 Curve fitting toolbox

The area under the graph of each absorbance spectrum was essential in determining the corresponding critical wavelength<sup>[7]</sup>. In order to calculate the area through numerical integration, equations were needed. Thus, the scatter data had to be fitted to a curve. This was done by using the Curve Fitting Toolbox<sup>[25]</sup>, a sub-application in MATLAB.

By selecting the data for the *x* (wavelength) and *y* (absorbance) axes from *uvb\_spectrum\_trial2\_110820.mat*, each compound's scatter data were fitted with distribution functions as seen in Figure 7, Figure 8, and Figure 9. Here, the absorbance of caffeic acid, gallic acid, and pinocembrin was fitted to a fifth order polynomial function, a fourth harmonic Fourier function, and a three-termed Gaussian function<sup>[26]</sup>, respectively.

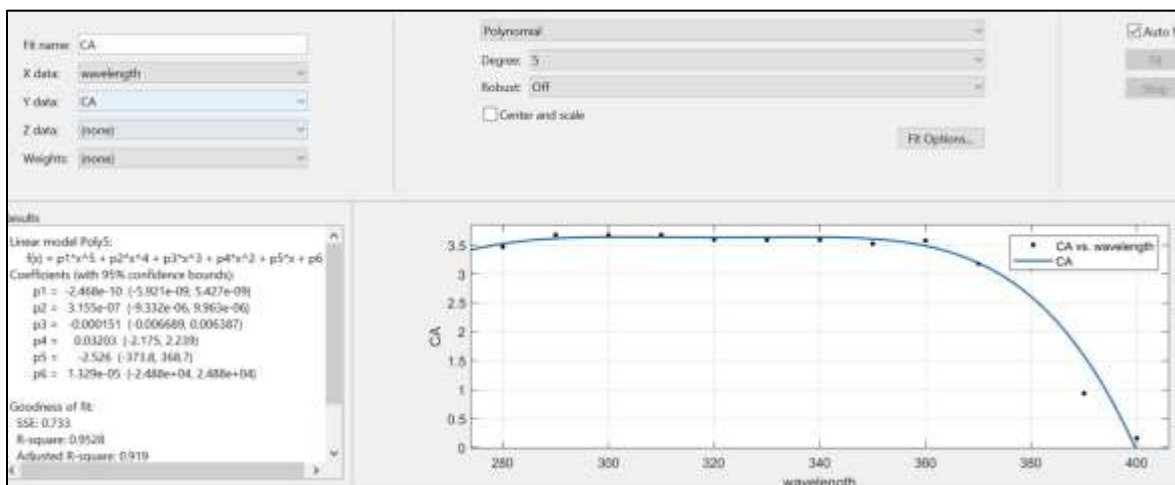


Figure 7. Fifth order polynomial fit for the scatter data of absorbance for caffeic acid.

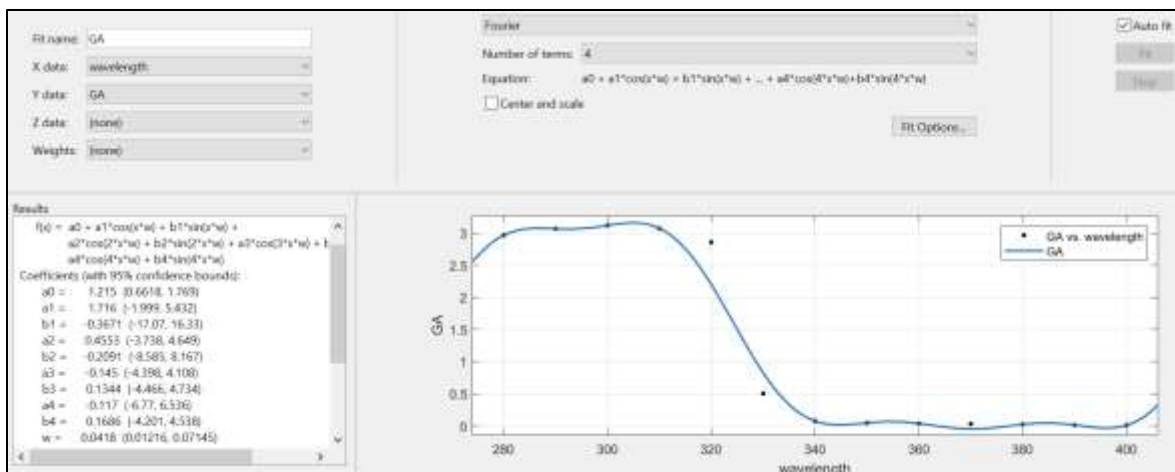


Figure 8. Fourth harmonic Fourier fit for the scatter data of absorbance for gallic acid.

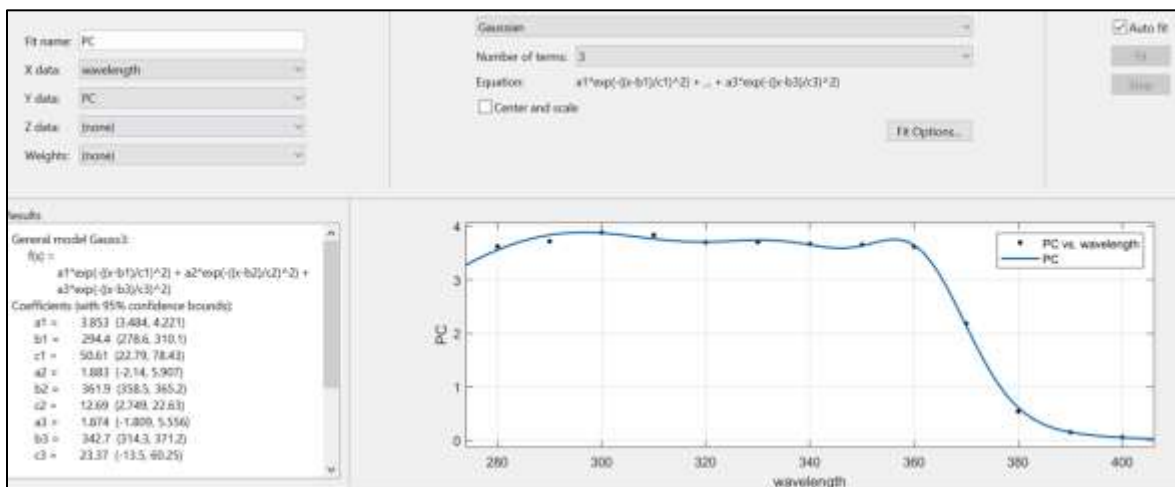


Figure 9. Three-degree gaussian fit for the scatter data of absorbance for pinocembrin.

From the Figures above, the fitting equation of caffeic acid can be written as Equation 2, Equation 3 and Equation 4 respectively:

$$f(\lambda) = p_1\lambda^5 + p_2\lambda^4 + p_3\lambda^3 + p_4\lambda^2 + p_5\lambda + p_6 \quad (2)$$

$$f(\lambda) = a_0 + a_1 \cos(\lambda w) + b_1 \sin(\lambda w) + a_2 \cos(2\lambda w) + b_2 \sin(2\lambda w) \\ + a_3 \cos(3\lambda w) + b_3 \sin(3\lambda w) + a_4 \cos(4\lambda w) + b_4 \sin(4\lambda w) \quad (3)$$

$$f(\lambda) = a_1 e^{-\left(\frac{\lambda-b_1}{c_1}\right)^2} + a_2 e^{-\left(\frac{\lambda-b_2}{c_2}\right)^2} + a_3 e^{-\left(\frac{\lambda-b_3}{c_3}\right)^2} \quad (4)$$

Whereby as functions of  $\lambda$ , the wavelength:  $p_1, p_2, p_3, p_4$ , and  $p_5$  are the coefficients for the polynomial equation;  $a_0, a_1, a_2, a_3, a_4, b_1, b_2, b_3, b_4$ , and  $w$  are the coefficients for the Fourier equation;  $a_1, a_2, a_3, b_1, b_2, b_3, c_1, c_2$ , and  $c_3$  are the coefficients for the Gaussian equation.

The fitness of the models was verified in terms of the low Root Mean Squared Errors (RMSE) and  $r^2$  coefficient of determinations having values close to unity as seen in Figure 10. Nevertheless, a high  $r^2$  value does not necessarily suggest a good fit. Therefore, visual verifications were also required. As such, the curve lines were plotted and compared with the scattered data in the MATLAB Editor as demonstrated in Figure 11.

| Table of Fits |                   |          |        |          |     |          |        |         |
|---------------|-------------------|----------|--------|----------|-----|----------|--------|---------|
| Fit name      | Data              | Fit type | SSE    | R-square | DfE | Adj R-sq | RMSE   | # Coeff |
| GA            | GA vs. wavelength | poly5    | 0.7330 | 0.9528   | 7   | 0.9190   | 0.3236 | 6       |
| GA            | GA vs. wavelength | fourier4 | 0.5467 | 0.9794   | 3   | 0.9175   | 0.4269 | 10      |
| PC            | PC vs. wavelength | gauss3   | 0.0321 | 0.9988   | 4   | 0.9965   | 0.0896 | 9       |

**Figure 10.** Table of fits showing the goodness of fit of the gaussian function for all compounds.

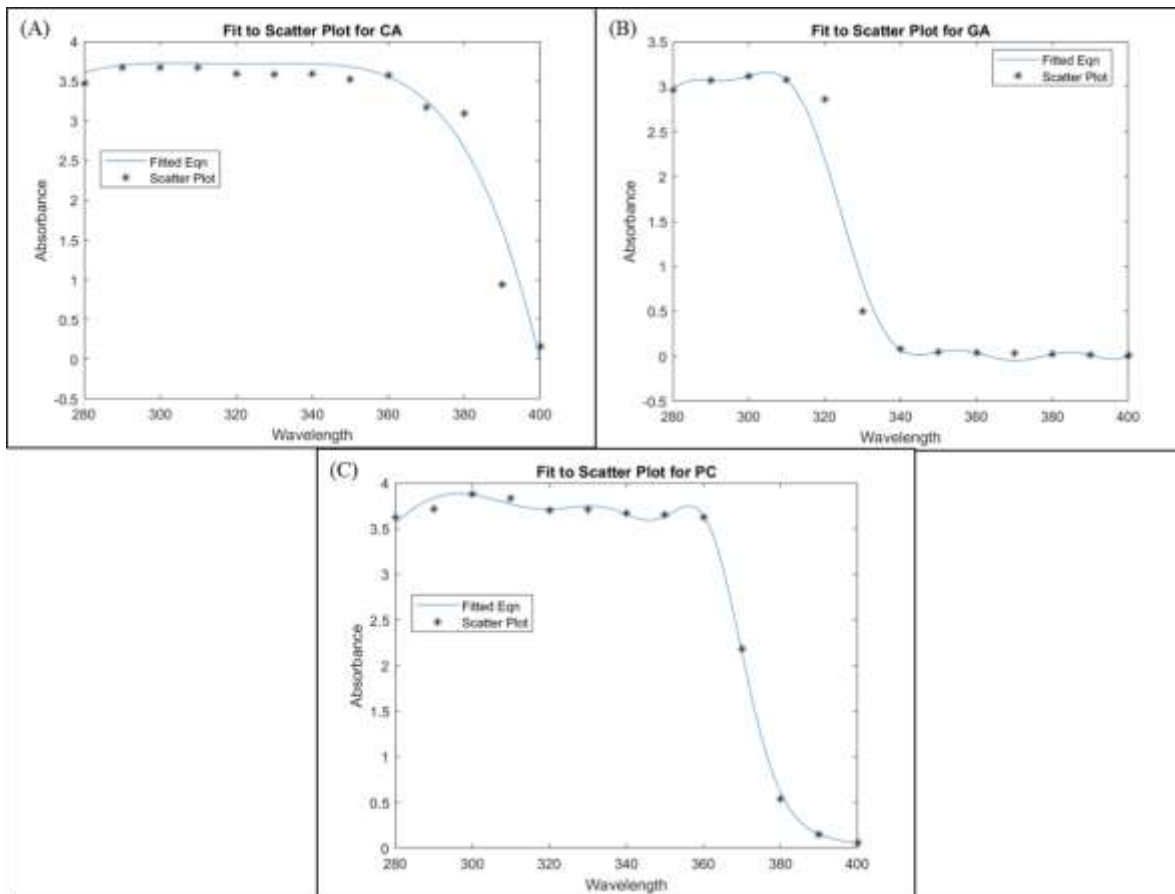


**Figure 11.** Visual verification for curve fitted to (A) caffeic acid, (B) gallic acid and (C) pinocembrin.

*2.3.4 MATLAB editor: Obtaining area under graph and pinpointing critical wavelengths*

With the fitted equations generated from the Curve Fitting Toolbox, the next step was to calculate the area under the graph by running the codes in the MATLAB Editor. The equations had to first be integrated. The user is expected to have the mathematical knowledge of integrating the equations manually. In this work, the integrals for the polynomial, Fourier, and Gaussian equation are shown in Equation 5 to Equation 8 respectively:

$$Integral(\lambda) = \int_{lower\ limit}^{upper\ limit} f(\lambda)d(\lambda) \tag{5}$$

$$\text{Polynomial Integral}(\lambda) = \frac{p_1\lambda^6}{6} + \frac{p_2\lambda^5}{5} + \frac{p_3\lambda^4}{4} + \frac{p_4\lambda^3}{3} + \frac{p_5\lambda^2}{2} + p_6\lambda \quad (6)$$

$$\begin{aligned} \text{Fourier Integral}(\lambda) & \quad (7) \\ & = a_0\lambda + \frac{a_1 \sin(\lambda w)}{w} - \frac{b_1 \cos(\lambda w)}{w} + \frac{a_2 \sin(2\lambda w)}{2w} - \frac{b_2 \cos(2\lambda w)}{2w} \\ & + \frac{a_3 \sin(3\lambda w)}{3w} - \frac{b_3 \cos(3\lambda w)}{3w} + \frac{a_4 \sin(4\lambda w)}{4w} - \frac{b_4 \cos(4\lambda w)}{4w} \end{aligned}$$

$$\text{Gaussian Integral}(\lambda) = -\frac{\sqrt{\pi}}{2} \left[ a_1 c_1 \cdot \text{erf} \left( \frac{b_1 - \lambda}{c_1} \right) + a_2 c_2 \cdot \text{erf} \left( \frac{b_2 - \lambda}{c_2} \right) + a_3 c_3 \cdot \text{erf} \left( \frac{b_3 - \lambda}{c_3} \right) \right] \quad (8)$$

These integrated equations were then passed in as function handles for each compound. The area under graph would then be the subtraction of the integration limits as seen in Equation 9 whereby the lower limit was the first recorded wavelength (in MATLAB syntax, *wavelength(1)*); and the upper limit was the last recorded wavelength, (in MATLAB syntax *wavelength(end)*).

$$\text{Area Under Graph} = \text{Integral}(\text{upper limit}) - \text{Integral}(\text{lower limit}) \quad (9)$$

As mentioned in Equation 1 the critical wavelengths occur at 90% of the integral with the 290-400 nm range. To find the critical wavelength,  $\lambda_c$ , the equation was rearranged into Equation 10 below such that it could be computed using numerical methods.

$$y(\lambda) = \{\text{Integral}(\lambda) - \text{Integral}(290)\} - 0.9\{\text{Integral}(400) - \text{Integral}(290)\} \quad (10)$$

$y(\lambda)$  denoted the solution for the critical wavelength, whereby  $\lambda_c$  was the value of  $\lambda$  that rendered  $y(\lambda)$  to be equals to zero.

The numerical method attempted here was the False-Position Method<sup>[27]</sup>, a commonly used closed root finding technique. Given the function handle,  $y(\lambda)$ , the lower bound, 290 nm, the upper bound, 400 nm, and the tolerance of the solution,  $\varepsilon$ , calling the function file, *false\_pos.m*, would use the False-Position Method to iteratively arrive at an estimate of the root of the equation, in this case, the critical wavelength, within the set precision or tolerance (0.001 was chosen here). The syntax for calling this function can be seen in the main script as “*root=false\_pos(y,290,400,0.001)*”. Note that the main script, also known as *m-file*, must be saved in the same folder as the function file.

### 3. Methods Validation

Next, the results were plotted in a graph with a red vertical line indicating the critical wavelength for each compound, as shown in Figure 12. The critical wavelength for caffeic acid

was calculated to be 378.2 nm, while gallic acid is 324.6 nm, and pinocembrin is 364.8 nm. Based on the critical wavelength obtained, it can be seen that although all three compounds were able to absorb within the UVB spectrum, only pinocembrin and caffeic acid were also able to absorb, until a certain extent, within the UVA spectrum. Caffeic acid itself even achieved beyond the critical wavelength of 370 nm, which is the wavelength where FDA and ISO had set as a benchmark for broad-spectrum sunscreens. When comparing with another study that had been done, García Forero, *et al.*<sup>[20]</sup> reported that pinocembrin and caffeic acid had a critical wavelength of 380 and 365 nm, respectively, which is slightly different from the results obtained in this study. However, this slight discrepancy could be due to the difference in calculating software, in which the authors did not specify or showcase the methods of calculation. As for gallic acid, no study had previously reported its critical wavelength even though it was reported to have photoprotective properties<sup>[23]</sup>. Hence, based on the current data obtained and the methods described here, the photoprotective coverage of the compounds can be ranked as such, caffeic acid > pinocembrin > gallic acid. This shows that caffeic acid and pinocembrin may be a much more suitable active ingredient to use in the formulation of a broad-spectrum sunscreen.

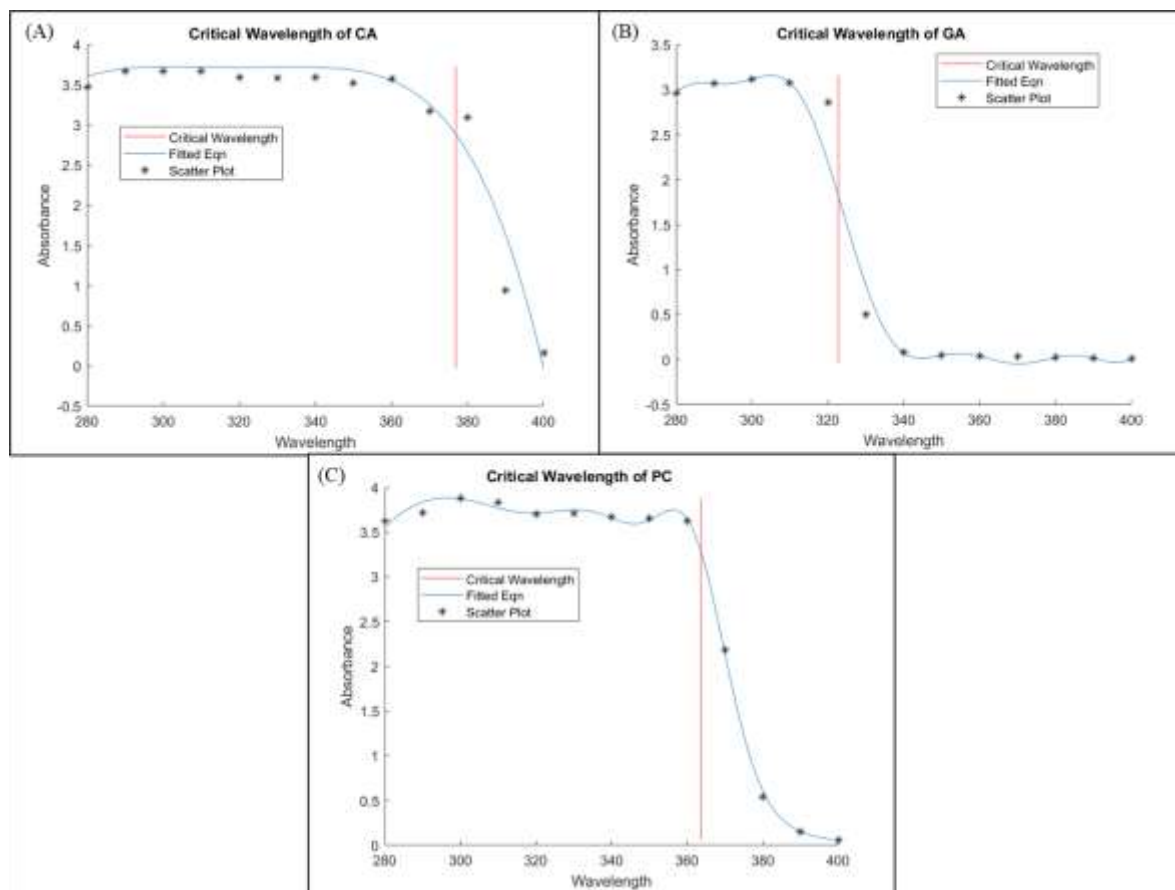


**Figure 12.** The critical wavelength of (A) caffeic acid = 378.2nm, (B) gallic acid = 324.6nm and (C) pinocembrin = 364.8nm.

Nevertheless, verifications were required. Here, the validity of the results was demonstrated by substituting the root back into  $y(\lambda)$ . If the answer is zero, the estimated root is verified as the critical wavelength. As can be seen in Figure 13, all the compounds obtained the value zero in their root validation, and thus, the critical wavelength calculated was deemed accurate.

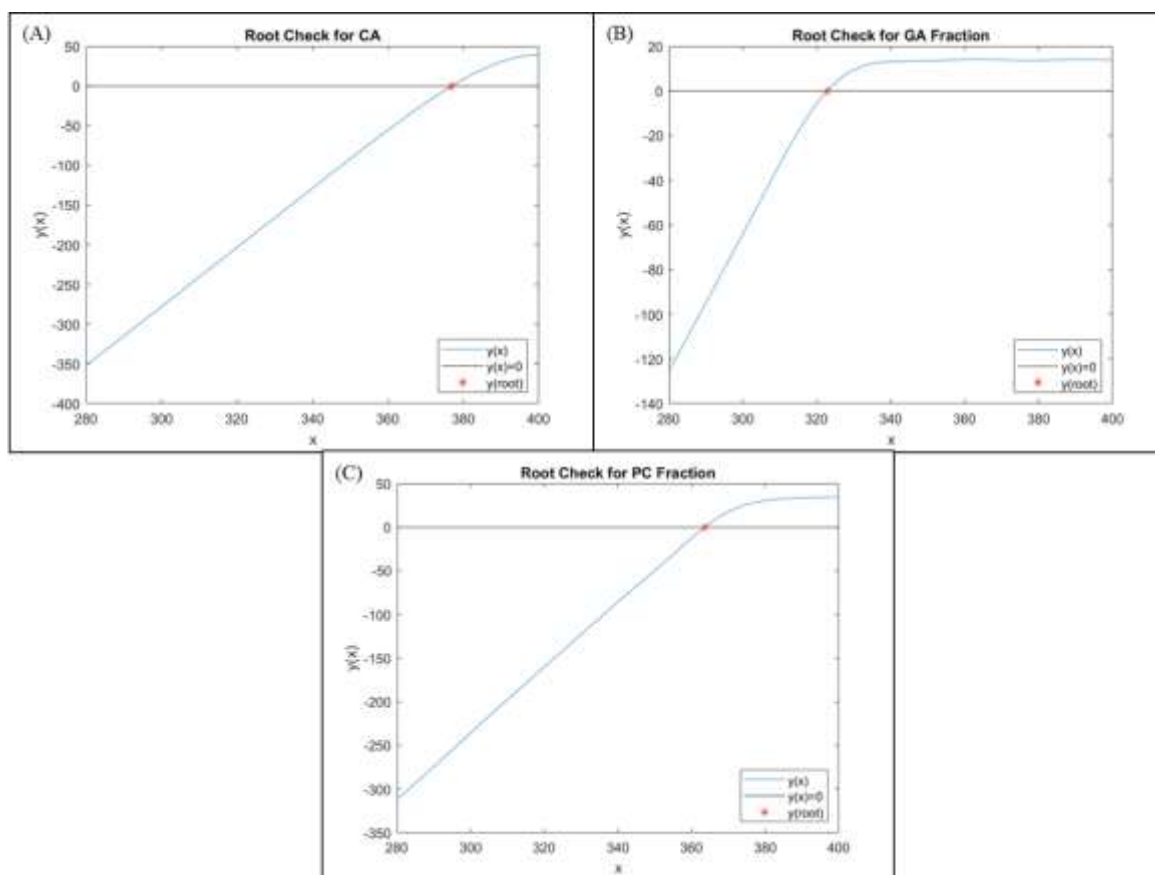


**Figure 13.** Root verification for (A) caffeic acid, (B) gallic acid, and (C) pinocembrin showing that the solutions obtained do indeed cause  $y(\lambda) = 0$ .

#### 4. Conclusions

In summary, the measurement of critical wavelength gives valuable insight on the potential photoprotective properties of a compound. Through this preliminary screening, cosmetic companies may be able to reduce the cost of compound testing for broad-spectrum sunscreens. In this work, explanations of the steps taken in Curve Fitting Toolbox and codes scripted in MATLAB Editor were relayed to assist any future researcher interested in determining the critical wavelengths. Starting from the installations of prerequisite software, fitting the experimental data to an analytical equation, to identifying the critical wavelength by calling the function file that performs numerical methods, all steps were explained with the aim of letting future researchers understand the execution process. This work was done with the hope

that researchers could simply edit the required inputs in the main script for different test cases, or even undertake similar approaches in determining critical wavelengths.

**Author Contributions:** Conceptualization, B.H.G. and Camille K.M.; methodology, Camille K.M. and C.K.M.; software, C.K.M.; validation, Camille K.M., C.K.M. and B.H.G.; formal analysis, Camille K.M. and C.K.M.; investigation, C.K.M.; resources, P.P., T.T.H., L.-H.C., B.H.G.; writing—original draft preparation, Camille K.M. and C.K.M.; writing—review and editing, Y.Y.Y., Y.K., T.M.K., A.D., P.P., T.T.H., L.-H.C., B.H.G.

**Funding:** This work was financially supported by External Industry Grants from Biotek Abadi Sdn Bhd (vote no. GBA-81811A), Monash Global Asia in the 21st Century (GA21) research grant (GA-HW-19-L01 & GA-HW-19-S02) and Fundamental Research Grant Scheme (FRGS/1/2019/WAB09/MUSM/02/1).

**Conflicts of Interest:** The authors declare no conflict of interest.

## References

1. Chung, JH. Photoaging in Asians. *Photodermatol. Photoimmunol. Photomed.* 2003; 19 (3): 109–121, doi:10.1034/j.1600-0781.2003.00027.x.
2. Rabe, JH, Mamelak, AJ, McElgunn, PJS, *et al.* Photoaging: Mechanisms and repair. *J. Am. Acad. Dermatol.* 2006; 55(1): 1–19, doi:10.1016/j.jaad.2005.05.010.
3. Thiyagarasaiyar, K, Goh, B-H, Jeon, Y-J, *et al.* Algae metabolites in cosmeceutical: An overview of current applications and challenges. *Mar. Drugs* 2020; 18(6), 323, doi: 10.3390/md18060323.
4. Antoniou, C, Kosmadaki, MG, Stratigos, *et al.* Sunscreens – what's important to know. *J. Eur. Acad. Dermatol. Venereol.* 2008; 22(9): 1110–1118, doi:10.1111/j.1468-3083.2008.02580.x.
5. Serpone, N, Salinaro, A, Emeline, AV, *et al.* An in vitro systematic spectroscopic examination of the photostabilities of a random set of commercial sunscreen lotions and their chemical UVB/UVA active agents. *Photochem. Photobiol. Sci.* 2002; 1 (12): 970–981, doi:10.1039/b206338g.
6. Diffey, BL, A method for broad spectrum classification of sunscreens. *Int. J. Cosmet. Sci.* 1994; 16(2): 47–52, doi: 10.1111/j.1467-2494.1994.tb00082.x
7. Diffey, BL, Tanner, PR, Matts, PJ, *et al.* In vitro assessment of the broad-spectrum ultraviolet protection of sunscreen products. *J. Am. Acad. Dermatol.* 2000; 43(6): 1024–1035, doi:10.1067/mjd.2000.109291.
8. Mahendra, CK, Tan, LT-H, Yap, WH, *et al.* An optimized cosmetic screening assay for ultraviolet B (UVB) protective property of natural products. *Prog. Drug. Discov. Biomed. Sci.* 2019; 2(1), 1–6, doi: 10.36877/pddbs.a0000021.
9. Pelizzo, M, Zattra, E, Nicolosi, P, *et al.* In vitro evaluation of sunscreens: An update for the clinicians. *ISRN dermatol.* 2012; 352135, doi:10.5402/2012/352135.
10. ISO. ISO 24444:2010 Cosmetics — Sun protection test methods — In vivo determination of the sun protection factor (SPF). Available online: <https://www.iso.org/obp/ui/#iso:std:iso:24444:ed-1:v1:en> (accessed on 2018).
11. FDA. Guidance for industry labelling and effectiveness testing: Sunscreen drug products for over-the-counter human use - small entity compliance guide. Available online: <https://www.fda.gov/drugs/guidancecomplianceregulatoryinformation/guidances/ucm330694.htm> (accessed on 2018).
12. Kim, SM, Oh, BH, Lee, YW, *et al.* The relation between the amount of sunscreen applied and the sun protection factor in Asian skin. *J. Am. Acad. Dermatol.* 2010; 62(2): 218–222, doi:10.1016/j.jaad.2009.06.047.
13. Schalka, S, Dos Reis, VMS, Cucé, LC. The influence of the amount of sunscreen applied and its sun protection factor (SPF): Evaluation of two sunscreens including the same ingredients at different concentrations. *Photodermatol. Photoimmunol. Photomed.* 2009; 25(4), 175–180, doi:10.1111/j.1600-0781.2009.00408.x.
14. Mahendra, CK, Tan, LTH, Pusparajah, P, *et al.* Detrimental effects of UVB on retinal pigment epithelial cells and its role in age-related macular degeneration. *Oxid. Med. Cell. Longev.* 2020; 2020: 1904178, doi:10.1155/2020/1904178.

15. Mahendra, CK, Tan, LTH, Lee, WL, *et al.* Angelicin—A furocoumarin compound with vast biological potential. *Front. pharmacol.* 2020; 11: 366, doi:10.3389/fphar.2020.00366.
16. Saija, A, Tomaino, A, Trombetta, D, *et al.* In vitro and in vivo evaluation of caffeic and ferulic acids as topical photoprotective agents. *Int. J. Pharm.* 2000; 199(1), 39–47, doi:10.1016/s0378-5173(00)00358-6..
17. Mahendra, CK, Abidin, SA, Htar, TT, *et al.* Counteracting the Ramifications of UVB Irradiation and Photoaging with *Swietenia macrophylla* King Seed. *Molecules* 2021; 26(7), 2000, doi:10.3390/molecules26072000.
18. Jeon, J, Sung, J, Lee, H, *et al.* Protective activity of caffeic acid and sinapic acid against UVB-induced photoaging in human fibroblasts. *J. Food Biochem.* 2019; 43(2), e12701, doi: 10.1111/jfbc.12701.
19. Kang, NJ, Lee, KW, Shin, BJ, *et al.* Caffeic acid, a phenolic phytochemical in coffee, directly inhibits Fyn kinase activity and UVB-induced COX-2 expression. *Carcinogenesis* 2009; 30(2), 321–330, doi:10.1093/carcin/bgn282.
20. García Forero, A, Villamizar Mantilla, DA, Núñez, LA, *et al.* Photoprotective and antigenotoxic effects of the flavonoids apigenin, naringenin and pinocembrin. *Photochem. Photobiol.* 2019; 95(4), 1010–1018, doi:10.1111/php.13085
21. Zhang, D, Huang, B, Xiong, C, *et al.* Pinocembrin inhibits matrix metalloproteinase expression in chondrocytes. *IUBMB Life* 2015; 67(1), 36–41, doi:10.1002/iub.1343.
22. Kilicaslan, D, Kurt, AH, Doğaner, A. Protective effects of pinocembrin and pinostrobin against hydrogen peroxide-induced stress in retina pigment epithelial cells. *Pharm. Chem. J.* 2020; 54, 788–796, doi:10.1007/s11094-020-02275-y.
23. Wang, L, Ryu, B, Kim, W-S, *et al.* Protective effect of gallic acid derivatives from the freshwater green alga *Spirogyra* sp. against ultraviolet B-induced apoptosis through reactive oxygen species clearance in human keratinocytes and zebrafish. *Algae* 2017; 32(4): 379–388, doi:10.4490/algae.2017.32.11.29.
24. Hwang, E, Park, S-Y, Lee, HJ, *et al.* Gallic acid regulates skin photoaging in uvb-exposed fibroblast and hairless mice. *Phytother. Res.* 2014; 28(12), 1778–1788, doi:10.1002/ptr.5198.
25. Mathworks. Curve Fitting Toolbox. Available online: [https://www.mathworks.com/help/curvefit/index.html?searchHighlight=curve%20fitting%20toolbox&s\\_tid=srchtitle](https://www.mathworks.com/help/curvefit/index.html?searchHighlight=curve%20fitting%20toolbox&s_tid=srchtitle) (accessed on 2020).
26. MathWorks. Gaussian Models. Available online: <https://www.mathworks.com/help/curvefit/gaussian.html> (accessed on 2020).
27. Chabert, JL. Methods of False Position. In: *A history of algorithms: From the pebble to the microchip.* Berlin, Heidelberg: Springer Berlin Heidelberg; 1999. p. 83–112, doi:10.1007/978-3-642-18192-4\_4.



Author(s) shall retain the copyright of their work and grant the Journal/Publisher right for the first publication with the work simultaneously licensed under:

Creative Commons Attribution-NonCommercial 4.0 International (CC BY-NC 4.0). This license allows for the copying, distribution and transmission of the work, provided the correct attribution of the original creator is stated. Adaptation and remixing are also permitted.